Initial progress with numerical modelling of scattered light in a candidate eLISA telescope

Shannon R. Sankar[1] **and Jeffrey C. Livas**[2]
[1] Universities Space Research Association
[2] National Aeronautics and Space Administration, Goddard Space Flight Center

E-mail: shannon.r.sankar@nasa.gov

Abstract. We report a numerical analysis of the scattered light from within the field of view of an eLISA-like full-duplex telescope and, by comparison to a nominal allowable scattered light specification, we place constraints on the permissible mirror surface roughness and contamination levels of the mirrors. Our analysis was performed with commercially available stray light software, typically used in non-interferometric imaging telescopes and we do not include polarization or coherent effects. This work therefore represents the early steps towards a more complete understanding of the scattered light budget.

Introduction

Designs of interferometric space-based gravitational wave observatories continue to evolve. However all designs require exchange of laser beams between vastly separated spacecraft. In order to achieve this optical link, a telescopic element is required to both expand the beam going towards the far spacecraft and efficiently collect the beam sent from that far spacecraft. Mass and volume requirements dictate that the same telescope be used for these two purposes. The nominal eLISA telescope design is operated in full-duplex configuration - transmitting a 1 W beam, while simultaneously receiving approximately 100 pW, where the power difference between the outgoing and incoming beams is due largely to diffraction over the inter-spacecraft distance. This disparity of beam powers means that backscatter from the high-power outgoing beam is the chief contributor to the telescope scattered light budget. If this scattered light possesses large spatial overlap with the local oscillator at the detector, any phase fluctuations from the scattered light can couple to the interferometric displacement measurement. Ultimately, this phase noise must be kept small, to avoid reducing the observatory sensitivity and masking the signal from a gravitational wave.

Using this argument of minimizing phase noise, Spector and Mueller [1] have placed constraints on the permissible scatter which, when rescaled to eLISA specifications, implies the permissible scattered light power seen by the detector must be below approximately 100 pW. It is very difficult to achieve this level of scatter in an on-axis telescope design due to a strong narcissus reflection from the secondary mirror. Off-axis designs have tilted optical elements, eliminating the direct narcissus. However, the non-zero surface roughness and surface contamination still couple the outgoing beam into the received mode. It is this aspect of the telescope that we have studied numerically. Our choice of scattered light modelling software is FRED by Photon Engineering LLC.

[1] To whom any correspondence should be addressed.

Content from this work may be used under the terms of the Creative Commons Attribution 3.0 licence. Any further distribution of this work must maintain attribution to the author(s) and the title of the work, journal citation and DOI.
Published under licence by IOP Publishing Ltd

Reference design

The design of the telescope plays a key role in determining the scattered light seen by the detector. For this work, we have studied a particular off-axis reflective design consisting of four curved mirrors, referred to as M1 (primary), M2 (secondary), M3 (tertiary) and M4 (quaternary). Figure 1 shows the optical layout. The details of the design formulation have been presented elsewhere [2], [3]. The telescope expands a 5 mm outgoing beam to a 200 mm beam, giving an overall afocal magnification of 40, and also possesses an internal focus located between M2 and M3.

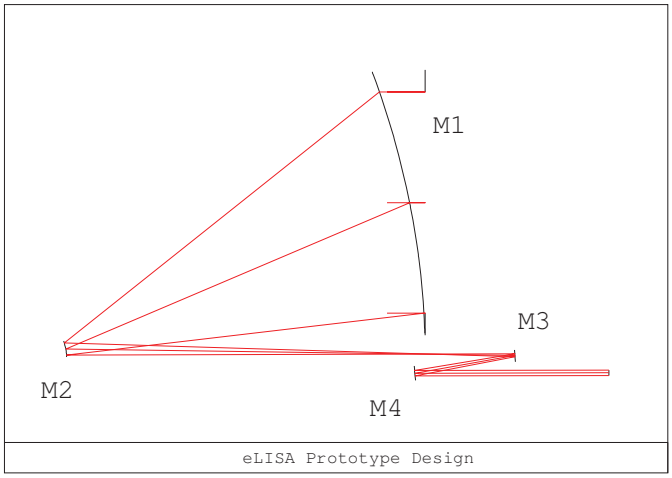


Figure 1. Scattered light was analysed using a 4-mirror, off-axis, afocal design template shown above.

Methodology for stray light calculation

In simulating the system, we chose to ignore scatter from structure or non-optical surfaces outside the field of view as separate estimates place those contributions several orders of magnitude below the scatter from the mirrors. The total stray light is then due to contributions from both particulate contamination and random residual surface errors of the mirrors. These two individual sources of scatter are addressed by the Mie scatter model and the Harvey-Shack scatter model, respectively. Both types of scatter are well implemented in most scattered light simulation software. FRED uses efficient algorithms for the calculation of the total scatter and also includes importance sampling, which greatly reduces the processing time and number of traced rays necessary for convergence of the scattered power.

Surface roughness properties ranging from 0.1 to 15 nm were applied to each mirror in turn. Similarly, particulate levels were varied on each mirror surface, simulating different cleanliness levels from CL100 to CL300 as defined by [4]. By iteratively changing these parameters on each surface and analysing the scattered power on the detector, it was possible to deduce the most relaxed parameters for which the specification of scattered power is still met.

We note that a key concept in the telescope scatted light model is the inclusion of a spatial and angular window, physically provided mainly by the overlap integral of the beams on the detector. To model this aspect of the system in a ray-tracing sense, we purposely restricted our interest to only include rays which impinge on the detector area within a small ±8 μrad circular field of view. This necessary restriction was implemented by explicitly coding an angular filter for the direction cosines of the incident rays, and rejecting scatter from outside this cone. We stress that this angular ray filter does

not include coherent effects or interference, which may alter the results. More work will be done in the future to better simulate the scatter using physical optics propagation and an explicit beam overlap. Polarization information, and the effect of polarization optics, was not explicitly included in this analysis. Furthermore, the scattered power from optical elements between the detector and M4 was not included, though the methodology is scalable enough that these optics may be included in future simulations. It should be noted that such optics may contribute scattered power but are expected to produce very little phase noise in the interferometric measurement, if they are located on the ultra-stable optical bench. Finally, the coherence effects among the scattered field, the signal field and the local oscillator field were not included, except in the formulation of the permissible scatter [1] as noted in the Introduction section.

Initial Results

The initial results from the telescope scatter simulation in FRED indicate that a sizeable fraction of the scatter at the detector for this design is due to M3 and M4. The M4 contribution is zeroth-order scattering, being generated by the quaternary mirror and going directly to the simulated detector. However, for this design, the scatter contribution from M3 is largest. Our simulations imply that this property is due to a focusing effect from M4 - the quaternary mirror position, orientation and curvature are such that it efficiently reflects the low-angle scatter generated by the tertiary mirror onto the detector - an example of first order scatter. Scatter from the primary and secondary mirrors is also directed to the detector in this manner, but the overall relay efficiency of scatter from those optics to the detector is smaller than it is for M3 in this design. Table 1 presents the total scattered power from each optic, along with the surface roughness and contamination levels used in the simulation.

Table 1. Scattered light on the detector due to each mirror with optimized specifications.

Mirror	Cleanliness Level[a]	Surface Roughness (nm)	Scattered Power on Detector[b] (W)
M1	CL 300	1.5	< 5e-14
M2	CL 200	1.5	2e-12
M3	CL 200	0.5	5e-11
M4	CL 200	0.5	9e-12

[a] Contamination levels are listed in accordance with [4]. Future model refinement will include more realistic particle distributions [5].
[b] Scattered power simulations are typically accurate to within a small factor of approximately 2 or 3.

It is important to note that the modelling shows that the majority of the scatter at this level is due to the particulate contamination, not the direct surface roughness of the optical surface. Deposited film contamination and/or non-volatile residue, such as hydrocarbons or water ice, have not been modelled here.

Outlook and Future Work

Rigorous testing in an experimental setting is required to address effects which are not modelled (such as polarization and coherence) and also to verify the effectiveness of the current model in analysing other contributions. To accomplish this goal, a full scale prototype telescope is being constructed. A direct test of the stray light will be performed and we anticipate a full comparison to the scattered light model. A smaller scale testbed will be used in the meantime to verify the model as it applies to the M3-M4 pair. We expect that the model will be refined in the future as we perform experimental tests of the scattered light power at the detector.

Acknowledgments
The authors wish to acknowledge the technical assistance provided by the Goddard Space Flight Center Optics Branch, particularly Lenward Seals, Garrett West and Joseph Howard. This work was supported by NASA Strategic Astrophysics Technology award 11-SAT11-0027.

[1] Spector A, Mueller G, 2012 *Class. Quantum Grav.* 29 205005
[2] Livas J, Sankar S, in preparation, to be submitted to the *Proceedings of the 10th LISA Symposium in Gainesville FL 2014*
[3] Livas J, Arsenovic P, Crow J, Hill P, Howard J, Seals L, Shiri S, 2013 *Opt. Eng.* 52(9). 091811.
[4] Military Standard MIL-1246C Particulate contamination
[5] Peterson R, Magallanes P, Rock D, 2002 *Proc. SPIE* 4774, Optical System Contamination: Effects, Measurements, and Control VII, 79